

Supporting Information

Iodine doping induced activation of covalent organic framework cathodes for Li-ion batteries

Guoying Ren ^a, Fengshi Cai ^{a*}, Shoucheng Wang ^a, Zhiqiang Luo ^{b*}, Zhihao Yuan ^c

a. Tianjin Key Lab for Photoelectric Materials and Devices, School of Materials Science and Engineering, Tianjin University of Technology, Tianjin 300384, China.

b. Key Laboratory of Display Materials and Photoelectric Devices (Tianjin University of Technology), Ministry of Education of China, Tianjin 300384, China.

c. National Demonstration Center for Experimental Function Materials Education, Tianjin University of Technology, Tianjin 300384, China.

* Corresponding authors: Fengshi Cai and Zhiqiang Luo

E-mail address: caifs@tjut.edu.cn; zhqluo@email.tjut.edu.cn

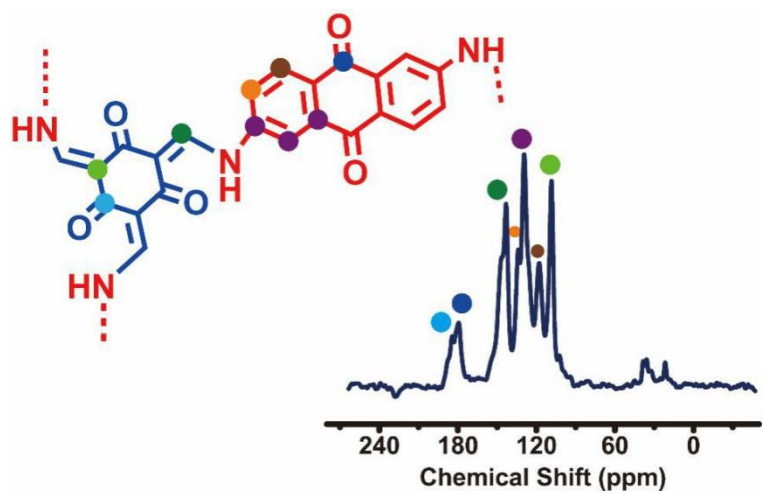


Figure S1. Solid-state ^{13}C NMR spectrum of COF. The corresponding carbons are labeled in the structural motif (inset).

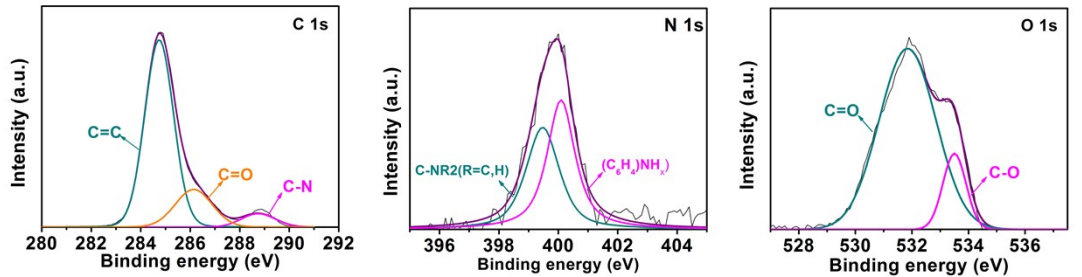
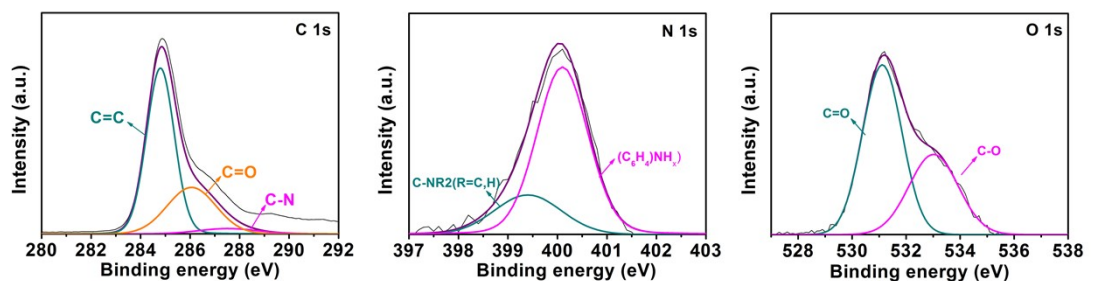
COF**COF-I**

Figure S2. C 1s, N 1s, and O1s high-resolution XPS spectra of COF and COF-I.

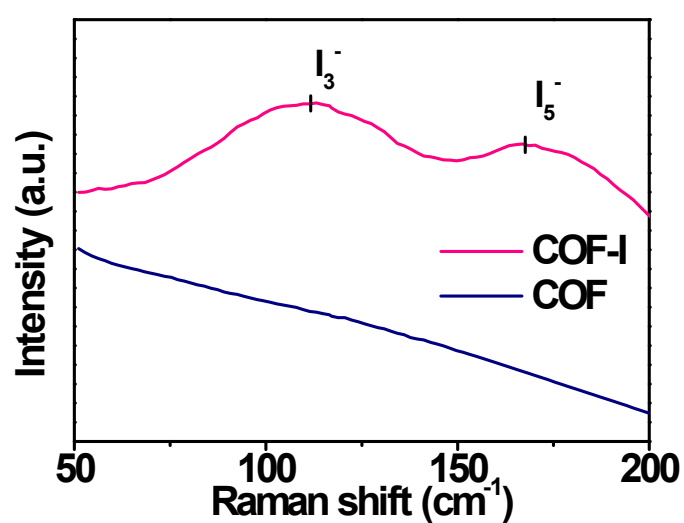


Figure S3. Raman spectra of COF and COF-I.

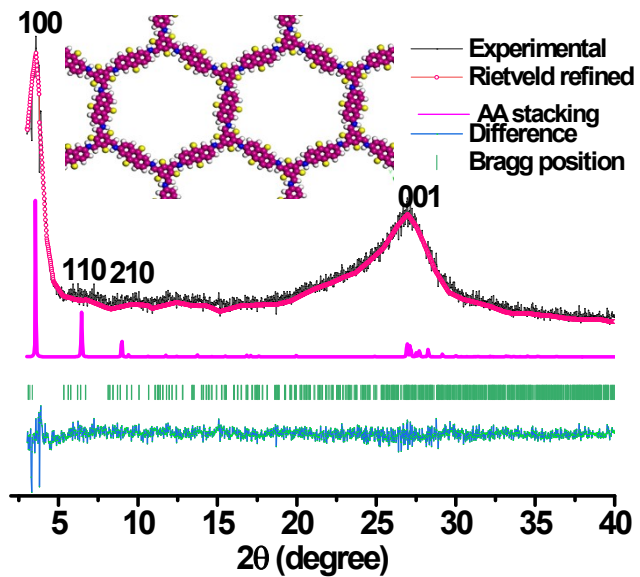


Figure S4. Experimental PXRD patterns, Pawley-refined patterns, simulated patterns, difference plots, Bragg positions for COF. The inset shows the simulated structure.

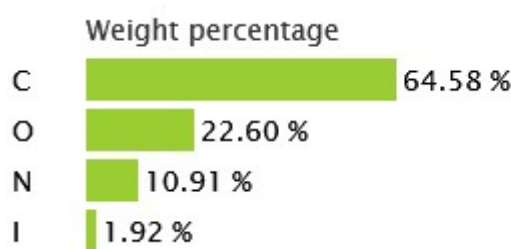
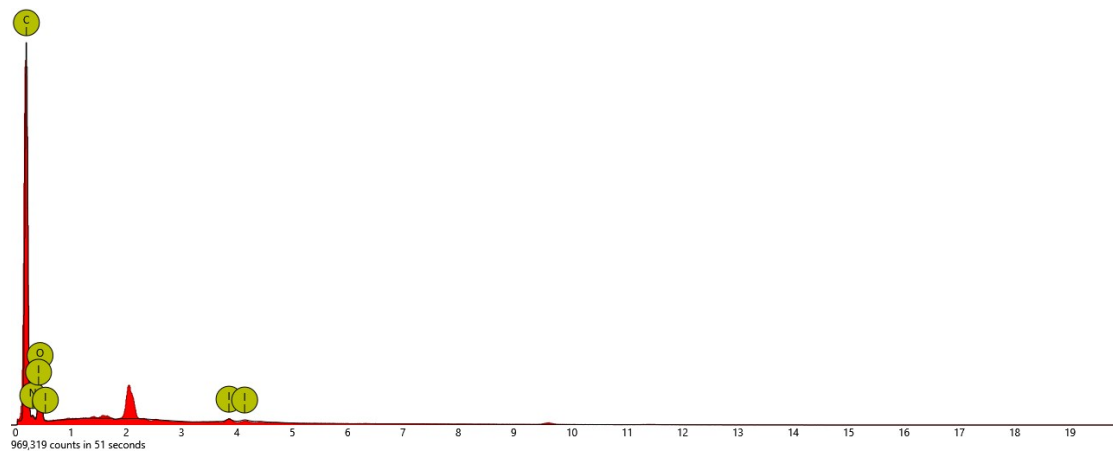


Figure S5. Energy-dispersive spectroscopy of COF-I.

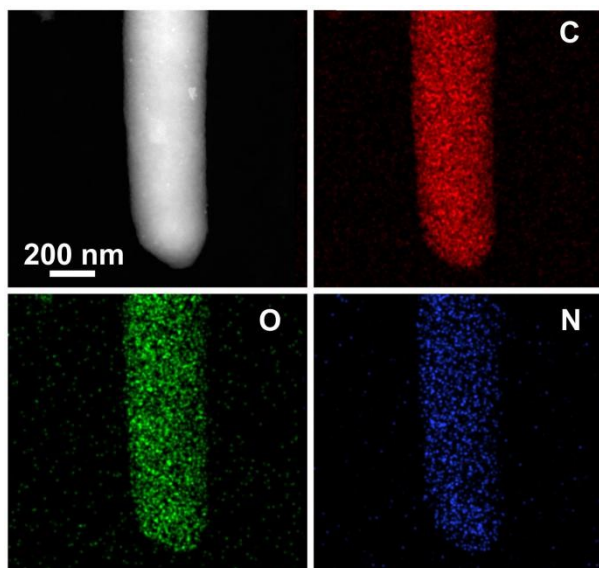


Figure S6. Energy-dispersive spectroscopy (EDS) elemental mapping images of C, N, O from the skeleton of COF. EDS images confirm the rodlike structure with a uniform distribution of C, N, O elements.

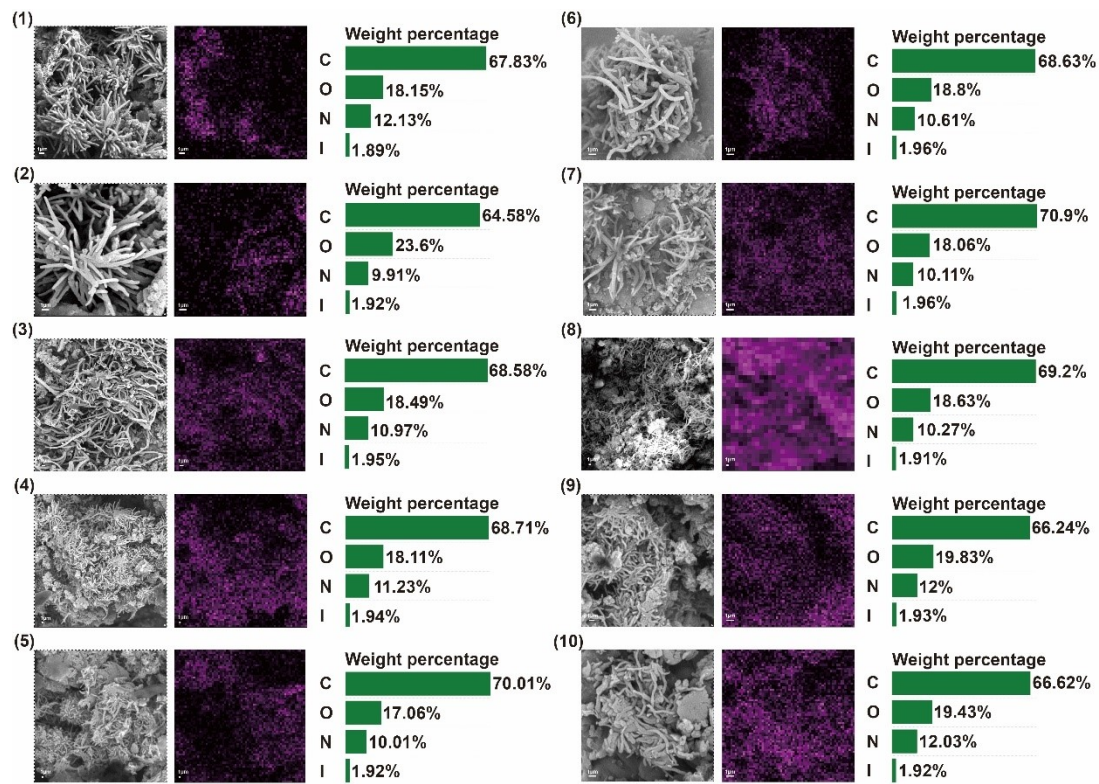


Figure S7. SEM images and the corresponding EDS for ten different batches of COF-I samples.

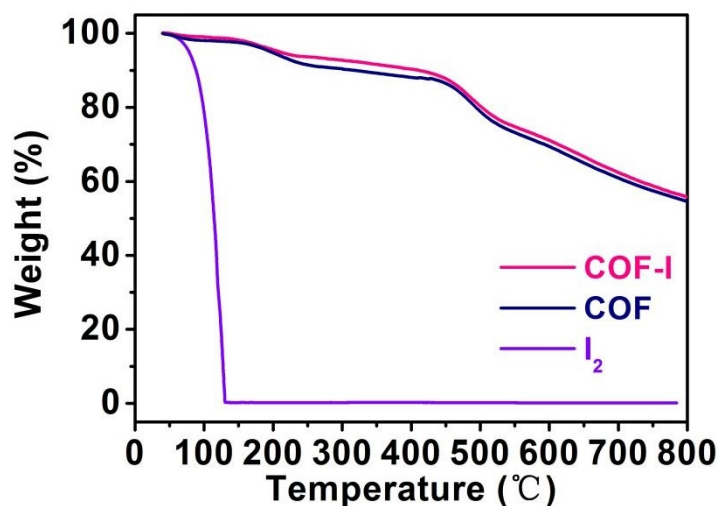


Figure S8. Thermogravimetric analysis curves of I₂, COF and COF-I.

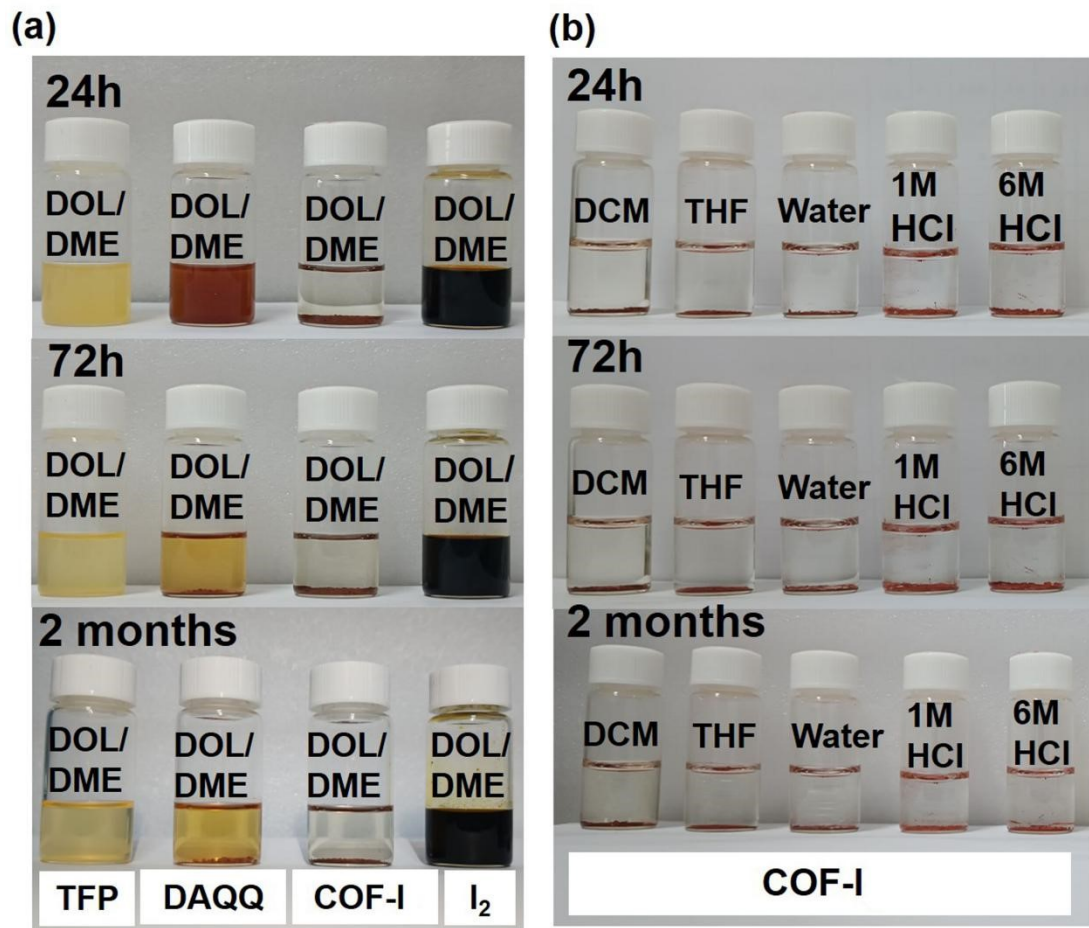


Figure S9. Chemical stability tests of COF-I in general solvents for 24h, 72h and 2 months.

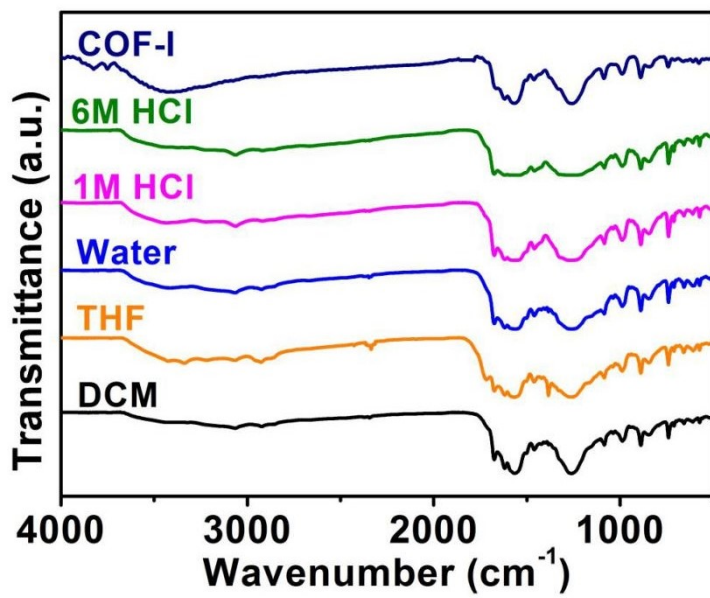


Figure S10. FT-IR spectra of COF-I after soaking in DCM, THF, water, 1M and 6 M HCl (aq.) for 24 hours.

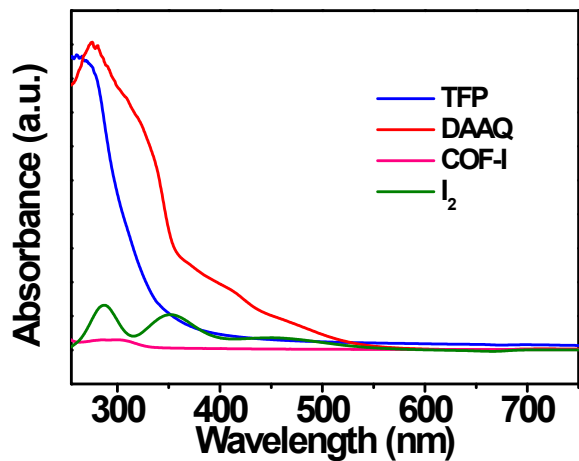


Figure S11. UV-vis absorption spectra of TFP, DAAQ, COF-I, I₂ after immersion treatments in 1,3-Dioxolane (DOL) / dimethoxyethane (DME) solvent for 2 months.

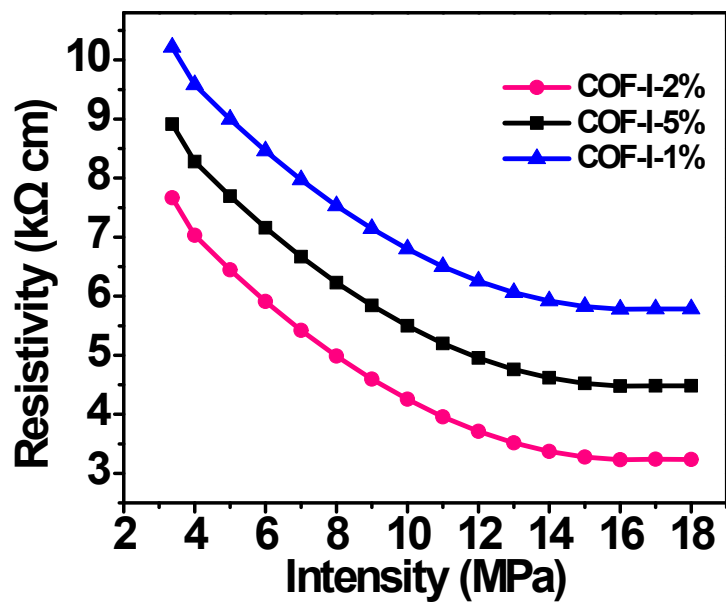


Figure S12. Relationship between pressure and resistivity for COF-I-1%, COF-I-2%, and COF-I-5%.

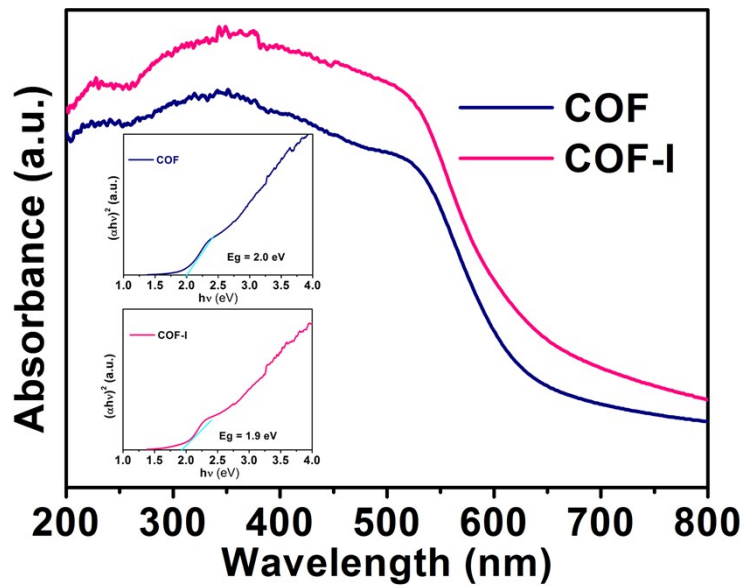


Figure S13. Solid-state UV-vis diffuse reflectance spectra for COF and COF-I. (inset) The corresponding K-M-transformed reflectance spectra.

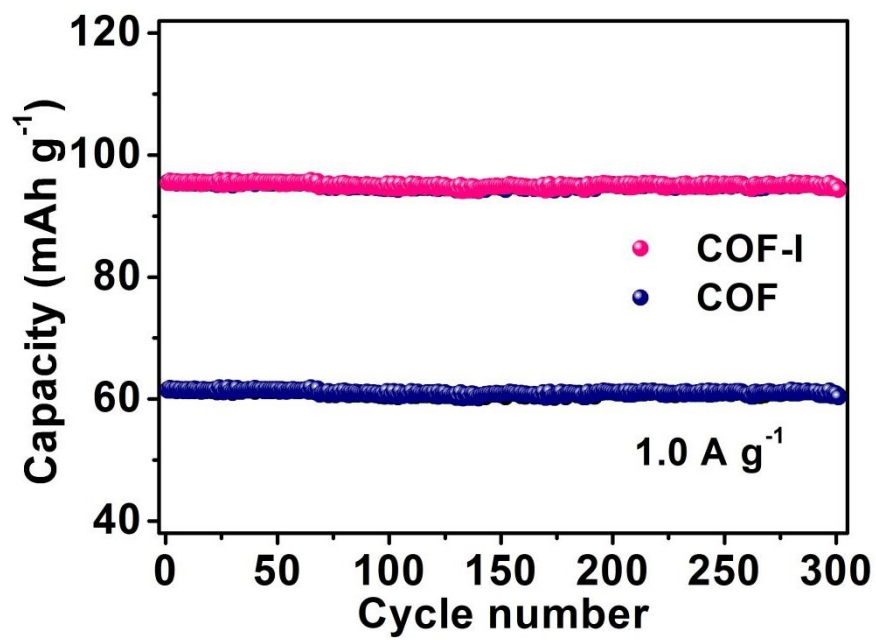


Figure S14. Cycling performances over 300 cycles at 1.0 A g^{-1} for COF and COF-I.

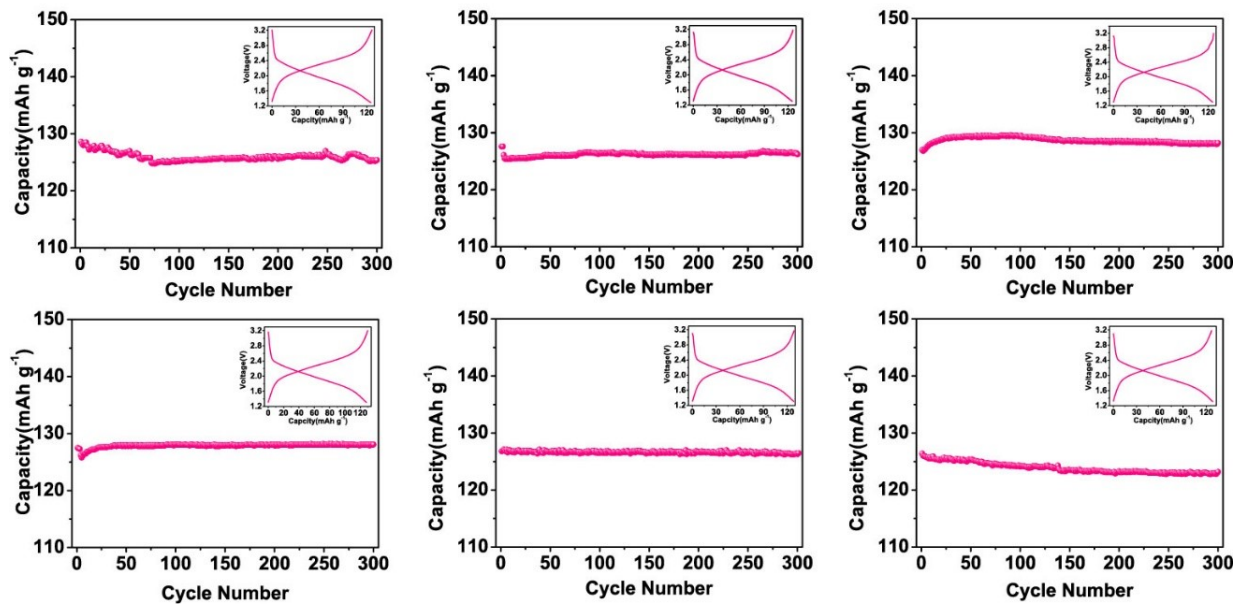


Figure S15. Cycling performances for six different batches of COF-I at 0.2 A g^{-1} .

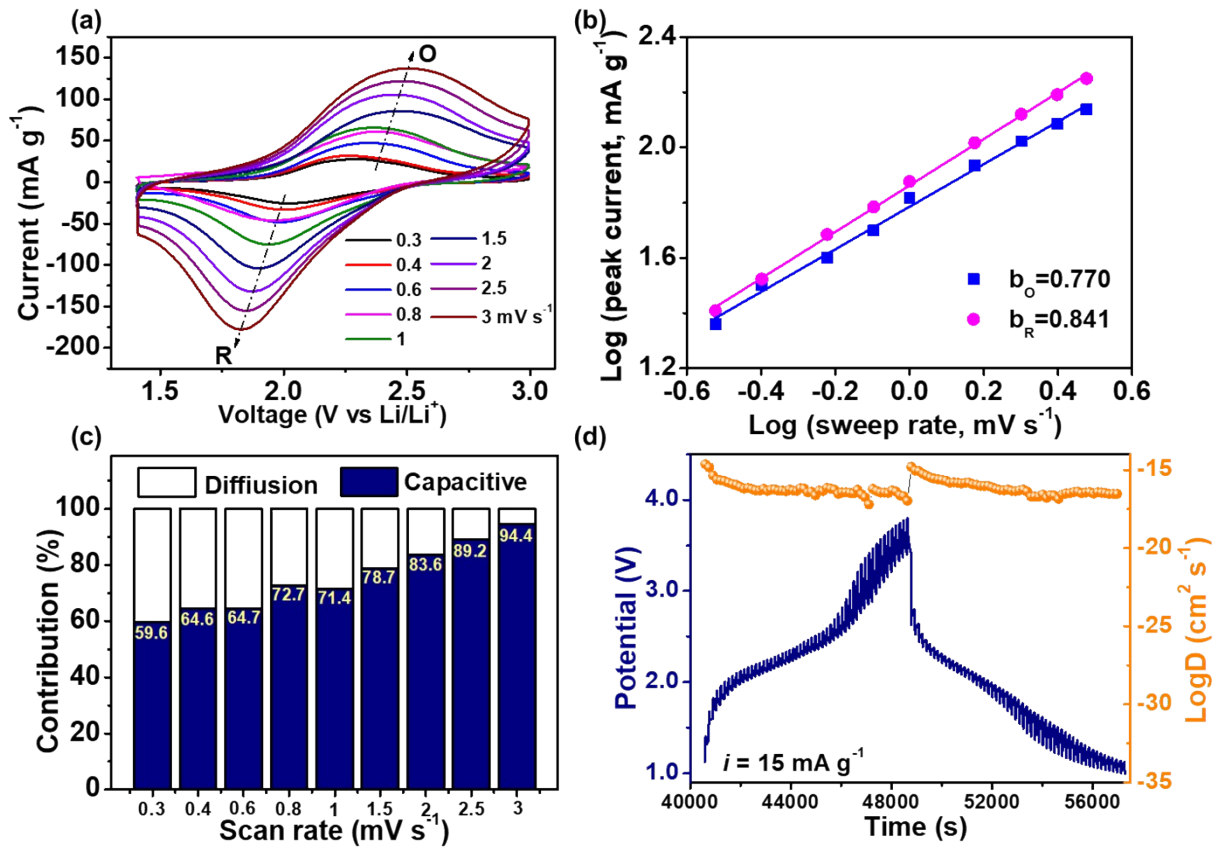


Figure S16. Kinetics analysis of COF. (a) CV curves obtained at different scan rates; (b) log (i) versus log (v) plots to determine the b values; (c) capacitive and diffusion contribution ratios to the total capacity at different scan rates; (d) GITT tests and corresponded ion diffusion coefficient of COF.

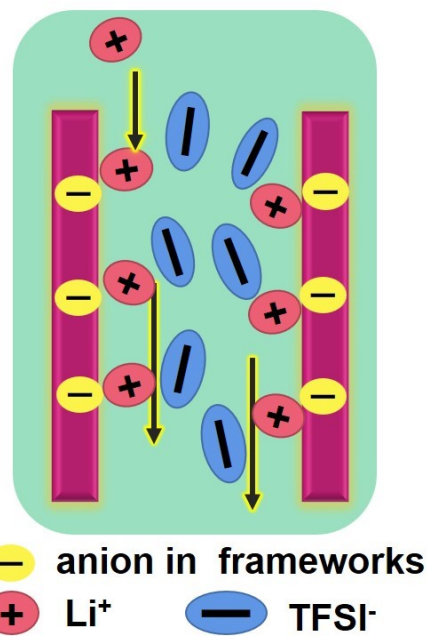


Figure S17. The diagram of Li^+ transport in COF-I.

Table S1. A comparison of the electrical properties of some previously reported COF materials at room temperature.

	COFs	Carrier mobility (cm ² V ⁻¹ s ⁻¹)	Carrier mobility after iodine doping (cm ² V ⁻¹ s ⁻¹)	Conductivity (S m ⁻¹)	Conductivity after iodine doping (S m ⁻¹)	References
1	DAAQ-COF	8.36	11.05	1.63×10 ⁻⁴	2.28×10 ⁻³	This work □
2	NiPc-CoTAA	0.15	-	8.16×10 ⁻³	0.52	[S1]
3	COF-DC-8	8.10	-	2.51×10 ⁻³	2.51	[S2]
4	TTF-COF	-	-	1.20×10 ⁻⁴	0.28	[S3]
5	POR-COF	-	-	4.6×10 ⁻⁹	1.52×10 ⁻⁵	[S4]
6	WBDT	-	-	2.7×10 ⁻⁴	4.72×10 ⁻²	[S5]
7	ZnPc-pz	4.80	22	7.0×10 ⁻⁵	3.1×10 ⁻²	[S6]
8	CuPc-pz	0.90	7	3.3×10 ⁻⁵	1×10 ⁻²	
9	TTF-ph-COF	0.2	-	-	1.00×10 ⁻³	[S7]
10	sp ² c-COF	-	-	6.1×10 ⁻¹⁴	7.10×10 ⁻²	[S8]
11	TANG-COF	-	-	1.6×10 ⁻³	0.15	[S9]
12	3D p-POP	-	-	5×10 ⁻⁸	2.9×10 ⁻⁵	[S10]
13	BUCT-COF-4	1.97	2.62	5.75×10 ⁻⁶	2.79×10 ⁻⁴	[S11]

References

- S1. Y. Yue, P. Cai, X. Xu, H. Li, H. Chen, H. Zhou and N. Huang, Conductive Metallophthalocyanine Framework Films with High Carrier Mobility as Efficient Chemiresistors, *Angew. Chem. Int. Ed.*, 2021, 60, 10806-10813.
- S2. Z. Meng, R. Stolz, and K. Mirica, Two-Dimensional Chemiresistive Covalent Organic Framework with High Intrinsic Conductivity, *J. Am. Chem. Soc.*, 2019, 141, 11929-11937.
- S3. S. Cai, Y. Zhang, A. Pun, B. He, J. Yang, F. Toma, I. Sharp, O. Yaghi, J. Fan, S. Zheng, W. Zhang and Y. Liu, Tunable electrical conductivity in oriented thin films of tetrathiafulvalene-based covalent organic framework, *Chem. Sci.*, 2014, 5, 4693-4700.

- S4. B. Nath, W. Li, J. Huang, G. Wang, Z. Fu, M. Yao and G. Xu, A new azodioxy-linked porphyrin-based semiconductive covalent organic framework with I₂ doping-enhanced photoconductivity, *CrystEngComm*, 2016, 18, 4259-4263.
- S5. J. Rotter, R. Guntermann, M. Auth, A. Mähringer, A. Sperlich, V. Dyakonov, D. Medina and T. Bein, Highly conducting Wurster-type twisted covalent organic frameworks, *Chem. Sci.*, 2020, 11, 12843-12853
- S6. M. Wang, M. Wang, H. Lin, M. Ballabio, H. Zhong, M. Bonn, S. Zhou, T. Heine, E. Canovas, R. Dong and X. Feng, High-Mobility Semiconducting Two-Dimensional Conjugated Covalent Organic Frameworks with p-Type Doping, *J. Am. Chem. Soc.*, 2020, 142, 21622-21627.
- S7. S. Jin, T. Sakurai, T. Kowalczyk, S. Dalapati, F. Xu, H. Wei, X. Chen, J. Gao, S. Seki, S. Irle, and D. Jiang, Two-dimensional tetrathiafulvalene covalent organic frameworks: towards latticed conductive organic salts. *Chem. Eur. J.*, 2014, 20, 14608-14613.
- S8. E. Jin, M. Asada, Q. Xu, S. Dalapati, M. Addicoat, M. Brady, H. Xu, T. Nakamura, T. Heine, Q. Chen and D. Jiang, Two-dimensional sp² carbon-conjugated covalent organic frameworks, *Science*, 2017, 357, 673-676.
- S9. V. Lakshmi, C. Liu, M. Rao, Y. Chen, Y. Fang, A. Dadvand, E. Hamzehpoor, Y. Sakai-Otsuka, R. Stein and D. Perekpichka, A Two-Dimensional Poly (azatriangulene) Covalent Organic Framework with Semiconducting and Paramagnetic States. *J. Am. Chem. Soc.*, 2020, 142, 2155-2160.
- S10. Y. Byun, L. Xie, P. Fritz, T. Ashirov, M. Dincă, A. Coskun, A Three-Dimensional Porous Organic Semiconductor Based on Fully sp²-Hybridized Graphitic Polymer. *Angew. Chem., Int. Ed.*, 2020, 59, 15166-15170.
- S11. S. Wang, X. Li, L. Da, Y. Wang, Z. Xiang, W. Wang, Y. Zhang and D. Cao, A Three-Dimensional sp² Carbon-Conjugated Covalent Organic Framework, *J. Am. Chem. Soc.*, 2021, 143, 15562-15566.